Two specific publications relevant to the work:

1. A unique water soluble probe for measuring the cardiac marker homocysteine and its clinical validation.(2022) Snehasish Debnath,Ratish R. Nair,Riya Ghosh, Gaddam Kiranmai,Narsini Radhakishan, **Narayana Nagesh*** and Pabitra B. Chatterjee*. *Chem Comm.*, 58, 9210 - 9213.

2. A Hydrogen Bonded Non-Porous Organic-Inorganic Framework for Measuring Cysteine in Blood Plasma and Endogenous Cancer Cell. (2024) Ghosh, Riya, Pradhan, Debjani, DEBNATH, SNEHASISH, Mansingh, Arushi, **Narayana Nagesh** * and Chatterjee, Pabitra*. *Chemistry - A European Journal,* DOI: 10.1002/chem.202401255, e202401255.

PAPER-1

ChemComm

ROYAL SOCIETY OF CHEMISTRY

COMMUNICATION

View Article Online
View Journal

Cite this: DOI: 10.1039/d2cc01515c

Received 16th March 2022,
Accepted 18th July 2022

DOI: 10.1039/d2cc01515c

rsc.li/chemcomm

A unique water soluble probe for measuring the cardiac marker homocysteine and its clinical validation†

Snehasish Debnath,[ab] Ratish R. Nair,[ab] Riya Ghosh,[ab] Gaddam Kiranmai,[c] Narsini Radhakishan,[d] Narayana Nagesh *[c] and Pabitra B. Chatterjee *[ab]

A series of copper(II) compounds 1–4 were synthesized and developed as fluorogenic probes to measure the cardiac marker homocysteine (Hcy) without any interference from other bioanalytes prevalent in human blood plasma including, cysteine and glutathione. UV-vis and EPR studies have provided confirmatory evidence for reduction-induced-emission-enhancement of the probe, which is responsible for the observed "off-to-on" behaviour towards Hcy. Water solubility, remarkable fluorescence enhancement (55–111 fold), and low detection ability (nearly 2.5 μM) make the probe suitable for clinical testing of cardiac samples. Investigation of 1 against a few reductive interferents testifies its specificity for Hcy. Results from clinical examination of cardiac samples by 1 when combined with the outcome of the reliability testing involving a clinically approved commercial immunoassay kit, validates the prospect of the molecular probe for direct measurement of Hcy in human plasma, which is unprecedented.

High concentrations (>15 μM) of the cardiac marker homocysteine (Hcy, Scheme S1, ESI†) in human plasma are accompanied by the early onset of several critical health illnesses and age related pathologies *viz.* atherosclerosis and thrombosis, acute coronary heart disease, ischemic stroke, early pregnancy loss, chronic renal dysfunction, microalbuminuria, cognitive impairment, Alzheimer's disease, and Parkinson's disease.[1] Consequently, measurement of plasma total homocysteine (tHcy) is obligatory for clinical supervision of various pathologies. Despite tens of thousands of publications in the literature on the relationship between Hcy and above-mentioned health disorders, very few Hcy selective optical probes exist in the literature.[2] Ever since Strongin *et al.* reported the optical method for selective detection of Hcy,[2a] not many reports are documented in the literature describing interference-free optical detection of Hcy (Table S1, ESI†). As clearly pointed out by Strongin and co-workers,[3] the obligatory requirement of non-aqueous media for the detection purpose has presumably made the clinical application of the Hcy-specific optical probes challenging. Wang *et al.* have recently developed a BODIPY-based complex for selective detection of Hcy in an aqueous medium.[2e] However, synthetic difficulty, cost of the reagents (*i.e.* BODIPY), and lack of detailed clinical validation and testing could be a major limitation in the development of optical assays using Wang's probe.[2e]

In this communication, we report the synthesis and characterization of four water-soluble (100% aqueous) copper compounds (1–4) to develop optical probes for measuring Hcy directly and selectively, in clinical samples. Upon addition of Hcy, non-fluorescent 1–4 showed 55–111 fold emission enhancement at physiological pH conditions, without any interference. Mechanistic studies have provided evidence for the preferential affinity of 1–4 towards Hcy. Herein, we demonstrate clinical testing of the Hcy-specific optical probe in a large number of human samples (cardiac patients and healthy volunteers as well). The performance of our presented assay has also been tested with a clinically approved immunoassay kit involving 60 clinical samples, which is unprecedented in the literature.

Yellow solids of the ligands HL_1–HL_4 were prepared from 7-hydroxycoumarin, as described in Scheme S2 (ESI†). The purity and molecular structures of HL_1–HL_4 and copper complexes (1–4) were established by C/H/N, IR, NMR, and ESI-MS (Fig. S1–S17, ESI†). Structural confirmation was gained from single crystal X-ray analyses (Fig. 1a and Fig. S13, Tables S2 and S3, ESI†). The structural index parameter τ (= 0.07), determined from the equation $\tau = (\beta - \alpha)/60$ (wherein, β and α are the two largest *L*–M–*L* angles),[4] indicates the square pyramidal geometry of the copper complex. Water-soluble 1–4 showed two weak absorption peaks as shoulders at 410 and 365 nm (Fig. S18, ESI†).

[a] *Analytical & Environmental Science Division and Centralized Instrument Facility, CSIR-CSMCRI, G. B. Marg, Bhavnagar, Gujarat, India. E-mail: pbchatterjee@csmcri.res.in*

[b] *Academy of Scientific and Innovative Research (AcSIR), Ghaziabad 201002, India*

[c] *Medical Biotechnology Complex, CSIR-CCMB, ANNEXE II, Hyderabad, Telangana, India. E-mail: nagesh@ccmb.res.in*

[d] *Department of Biochemistry, Nizam's Institute of Medical Sciences, Punjagutta, Hyderabad, Telangana, India*

† Electronic supplementary information (ESI) available: Materials and methods, synthesis, characterization data, Fig. S1–S53, Schemes S1–S3 and Tables S1–S7. CCDC 2105918–2105921. For ESI and crystallographic data in CIF or other electronic format see DOI: https://doi.org/10.1039/d2cc01515c

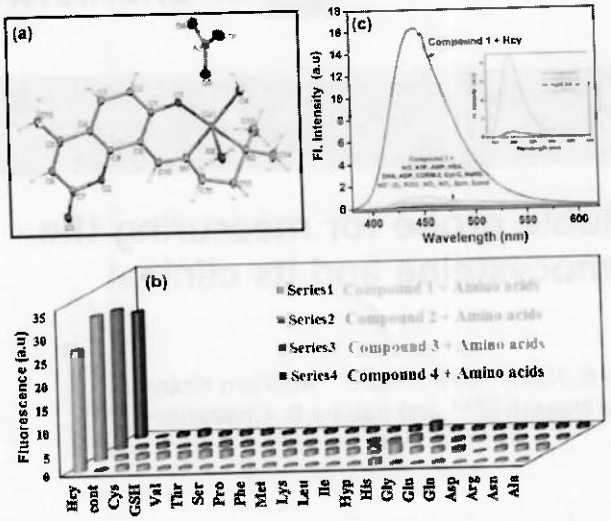

Fig. 1 (a) ORTEP view and atom-numbering scheme of the copper compound 1. (b) Fluorimetric responses of 1–4 (20 μM) toward different amino acids upon excitation at 370 nm in aqueous HEPES buffer solution (10 mM) at physiological pH (7.4). (c) Fluorescence responses of 1 (20 μM) towards other biologically relevant species (125 μM). Inset: Fluorescence of 1 (20 μM) towards variable concentrations of NaHS.

Furthermore, the complex displayed a d–d band at 625 nm (ε, 160 L mol^{-1} cm^{-1}). Because of the unique physical properties, high quantum yield, and great binding ability towards various analytes, coumarin derivatives have been found as fantastic fluorophores in the literature.[5] As a result of C=N isomerisation and/or electron transfer processes,[6] HL_1–HL_4 are weakly fluorescent (Φ_f = 0.01–0.014). However, complexes 1–4 are non-luminescent. The high binding affinity of Cu^{2+} towards ONN donor sites of HL_1–HL_4 further restricts the hydrolysis of 1–4 at neutral pH,[7] which has been confirmed from the pH profile (*vide infra*).

Emission behaviour of 1–4 against different amino acids is shown in Fig. 1b and Fig. S19 (ESI†), which revealed a large luminescence enhancement upon addition of Hcy with the formation of cyan colour (Fig. S20, ESI†). To check the efficacy of the probes for clinical applications, pH-variable luminescence measurement of 1–4 was explored further (Fig. S21–S24, ESI†). Throughout the pH regime, 1–4 remained non-fluorescent. To our surprise, emission spectra of 1–4 with Hcy showed maximum fluorescence at physiological pH. Hence, the working pH was found to be 6.5–8 (Fig. S21–S24, ESI†). All spectral experiments were performed with aqueous HEPES buffer (100% water) at physiological pH. We further have investigated the time-response behaviour of 1 in presence of Hcy. Results shown in Fig. S25 (ESI†), discloses that the luminescence intensity of 1 reaches a maximum within 60–70 min incubation with Hcy. Cys initially shows a little turn-on response. However, after 7–8 min incubation, the solution turned non-fluorescent. Luminescence spectra of 1–4 were measured after incubation of the probes with various amino acids and GSH for 30 min. A sharp 55–111 fold fluorescence increase was observed with Hcy. Thus, demonstrating Hcy selective nature of 1–4. The quantum yields were estimated to be within 0.134 to 0.091, much higher than the ligands. Thus, indicating adduct formation between Hcy and probes, instead of the replacement of the iminocoumarin ligand from the probes. From the Job's plot, the binding stoichiometry was found to be 1 : 1 (Fig. S26, ESI†). Without any interference, 1–4 responded to Hcy, even in presence of Cys and GSH (Fig. S27–S30, ESI†). Interference of Hcy congeners, *i.e.* Cys and GSH, have also been tested in different stoichiometric mixtures of them with Hcy. Results displayed in Fig. S31 (ESI†) reveals non-interference from Cys and GSH during the detection of Hcy. From fluorescence titration (Fig. S32–S35, ESI†), the calculated binding constants were found to be in the range 1.23–2.15 × 10^3 M^{-1} (Fig. S36, ESI†). The limit of detection (LOD) was calculated (Fig. S37, ESI†) to be in the order of 2.5 μM (compound 2), which is below the normal level of Hcy in healthy human blood plasma. Linearity within 0–100 μM supports the suitability of 1–4 at low concentration. Remarkable specificity of the probe towards Hcy is further reinforced when 1 was screened against a range of important bioanalytes (Fig. 1c). Furthermore, using varying concentrations of NaHS and other sulfur containing interferents that are commonly present in blood plasma, the non-emissive nature of the probe did not change (inset, Fig. 1c and Fig. S38, ESI†).

Reversible detection of Hcy by the probes (Fig. S39, ESI†) clearly demonstrates that the displacement of the ligand by the incoming Hcy ligand is not happening in 1–4. Thus, not in line to the proposal of Kim *et al.*[7] This could be the result of the redox reaction between probe and Hcy, wherein, Hcy reduces Cu(II) to Cu(I) at physiological pH. Upon deprotonation, Hcy binds Cu(I). Therefore, a ternary Cu(I) complex is formed. ESI-MS of 1, when recorded after half an hour of incubation with Hcy, showed a molecular ion peak of the intermediate ternary species at m/z = 512.58. This clearly implies the formation of the intermediate Cu(I) species, as shown in Fig. S40 (ESI†). Presumably, the reduction of Cu(II) is responsible for the fluorimetric "off-to-on" responses of 1–4 with Hcy. On the contrary, Cys with one less methylene group (Scheme S1, ESI†), initially showed a turn on response, which quickly diminished over time. After 7–8 min incubation, the solution mixture quenched completely. The pK_a value of the sulfhydryl group of Cys (8.00) is lower than that of Hcy (8.87).[8] As a result, Cys deprotonates faster than Hcy at physiological pH and it exists predominantly in the thiolate form. The isoelectric points of Hcy and Cys are 5.65 and 5.02, respectively.[9] Hence, both Hcy and Cys exist as negatively charged species at physiological pH. With Cu(II), Cys reacts faster than Hcy, resulting in the formation of a kinetically unstable 5-membered ring (as shown in Scheme S3, ESI†). The sulfhydryl group of Hcy deprotonates at a relatively slower rate than Cys. The deprotonated Hcy undergoes complexation with Cu(II) to form a kinetically favoured six membered ring. In both cases, a distinct fluorescence was initially observed upon addition of Hcy or Cys to the aqueous solutions of 1–4. This could be presumably due to the reduction of Cu(II) to Cu(I), which subsequently disrupts the PET process causing restoration of the fluorescence intensity. Interestingly, the fluorescence intensity of the probe was dramatically quenched for Cys after 8 min incubation. Whereas, it reaches a plateau after 60 min incubation with Hcy (Fig. S25, ESI†). In case of Cys, the

unstable five membered ring is not kinetically favoured. Hence, following the decomplexation of Cys, Cu(I) quickly gets oxidized to Cu(II) by the dissolved oxygen in the medium.[10]

The electronic spectrum of **1** (Fig. 2a) displays a d–d band at 625 nm.[11] Upon addition of Hcy, the band disappeared suggesting the formation of Cu(I) species. Supplementary experimental evidence in support of the above mentioned redox mechanism is also revealed from EPR studies. As expected, in the absence of Hcy, **1** displayed a 4-line EPR spectrum with g values, $g_{\parallel}$ = 2.141 and $g_{\perp}$ = 2.044.[12] On addition of Hcy to **1**, EPR of the mixture turned silent (Fig. 2b). Clearly, the reduction of Cu(II) with Hcy is supported by EPR. Time dependent fluorescence of **1** with variable concentrations of Hcy/Cys was further explored to support the mechanism. Separate kinetic investigations of **1** with Hcy and Cys were performed at 7.4 pH. Following pseudo first order kinetics, the change in fluorescence intensity has been fitted against time following the equation mentioned in the literature.[13] Initial kinetic data of **1** (20 μM) with 500 μM Hcy/Cys is shown in Fig. S25 and S41 (ESI†). The observed rate constants (k_{obs}) are 0.039 and 1.73 min^{-1} for Hcy and Cys, respectively (Fig. S41–S43, ESI†). Clearly, the k_{obs} values hint at a faster reaction rate of Cys than Hcy, as already revealed in the earlier section. Interestingly, the short half-life ($t_{1/2}$) of Cys (0.40 min) further confirms the instability of the five membered ternary intermediate compared to the six membered conjugate with Hcy (1-Hcy adduct, $t_{1/2}$ = 17.77 min). The kinetic profile of **1** towards variable concentrations of Hcy was examined next (Fig. S42, ESI†). The observed rate constant (k_{obs}) values were calculated to be 0.039, 0.043, 0.082, and 0.204 min^{-1} for 500, 250, 100, and 50 μM Hcy, respectively (Fig. S43, ESI†). The $t_{1/2}$ values for 500, 250, 100 and 50 μM Hcy were found to be 17.77, 16.11, 8.45, and 3.4 min, respectively. The increase in the half-life value with a rise in the Hcy concentration undoubtedly confirms the kinetic stability of the intermediate at a higher concentration regime.

Finally, time correlated single photon counting (Fig. S44–S47, ESI†) showed a decrease in the fluorescence lifetime (τ) of **1** from 5.58 ns to 5.15 ns upon addition of Hcy (Table S5, ESI†). Radiative (k_r) and total non-radiative (k_{nr}) rate constants are given in Table S5 (ESI†). Higher k_{nr} values of **1–4** (Table S5, ESI†) presumably refer to the photoexcited electron transfer (PET) processes occurring in **1–4**.[14] This event has ultimately resulted in the low k_r values, which is reflected in the observed non-emissive nature of **1–4**. From Table S5 (ESI†), it is clear that the key factor for fluorescence enhancement of **1–4** with Hcy is k_r. Therefore, addition of Hcy to the probe's solution has resulted in the drop of the non-radiative deactivation pathway (*i.e.* quenching of the PET process).[14] As discussed earlier, binding of Hcy to Cu(II) reduces the metal center, which ultimately inhibits the PET process causing fluorescence enhancement of the probes with Hcy. In other words, reduction-induced-fluorescence-enhancement of the probes has resulted in the development of an optical method for the direct measurement of Hcy in aqueous samples.

Surprisingly, Hcy selective probes reported hitherto in the literature are not water-soluble. Table S1 (ESI†) seems to suggest that Hcy specific organic probes are hydrophobic in nature. However, metal complex derived probes are ionic, as described in this work and earlier by Li *et al.* Therefore, the ionic complexes would be a good choice for developing water-soluble probes.[2e] Validation and clinical testing of the probes are two key studies that are indispensable to ascertain the usability and prospects of the developed optical probes for biomedical research. Observation from Table S1 (ESI†) reveals that researchers have under-investigated this aspect while developing Hcy-specific probes. Herein, we sought to validate **1** with the HPLC method first. For this purpose, different concentrations of Hcy were derivatized with thiol selective UV labelling reagent.[15] A linear calibration plot (ranging 5–100 μM) was generated by plotting the ratio of peak area of Hcy to internal standard (IS) *versus* concentration of injected Hcy (Fig. 3a). A few representative chromatograms are shown in Fig. S48 and S49 (ESI†). To validate our assay, two unknown concentrations of Hcy were prepared from 100 μM stock solution. The concentrations of the unknown Hcy solutions were then measured by the fluorescence technique (Fig. 3b) using **1** as well as by the HPLC method (Fig. 3a). The experimentally measured values by both the techniques compare considerably with an error percentage of 2 (Table S6, ESI†). Hence, the results validates the optical sensor reported in this work.

To carry out the real-world application of **1** for early diagnostic drive, we tested **1** for direct measurement of Hcy in the blood plasma of a good number of cardiac patients. Retention of the 4 line EPR of **1** for more than half a day indicates the stability of the probe in blood plasma (Fig. S50, ESI†). Kinetic experiments were also performed in blood plasma (Fig. S51, ESI†). It reveals fluorescence regeneration of **1** on addition of Hcy to the quenched plasma sample. This implies the non-displacement of the Cu ion from iminocoumarin ligand even in blood plasma.

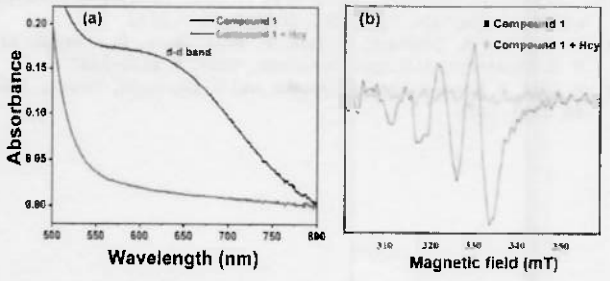

Fig. 2 (a) UV-vis spectra of **1** in the presence (blue line) and absence (red line) of Hcy (1 mM) in aqueous solution. (b) EPR spectra of **1** in the presence (black line) and absence (yellow line) of Hcy in an aqueous solution.

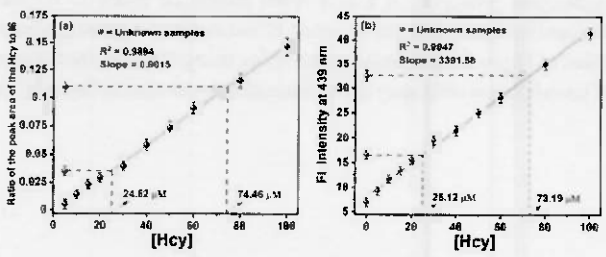

Fig. 3 Measurements of unknown concentrations of Hcy (a) using HPLC technique and (b) utilizing the linear fluorimetric calibration curve of **1** with Hcy in HEPES buffer solution (10 mM, pH = 7.4).

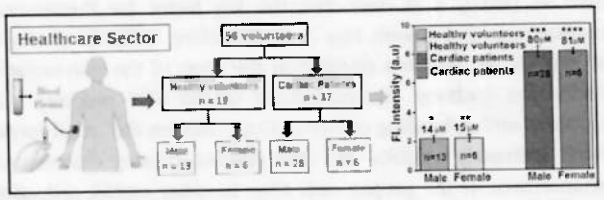

Fig. 4 Schematic representation showing Hcy levels measured by **1** in the blood samples of cardiac patients and healthy volunteers. In all cases (*, **, ***, and ****) $P < 0.05$. Each data point represents the average of triplicates.

Results from cytotoxicity studies of **1** and related Cu(I) species suggested no obvious toxicity (Fig. S52, ESI†). We next undertook the unique challenge of clinical investigation of **1**, which could be a potential candidate for point-of-care use. As expected, the fluorescence intensity of **1** was significantly lower in healthy volunteers than cardiac patients (Fig. 4). The total Hcy levels measured in the healthy volunteers were found to be in the range 09–17 μM and 10–16 μM in male and female categories, respectively. Meanwhile, the plasma tHcy levels in cardiac patients were calculated to be 70–82 μM and 74–80 μM in male and female samples, respectively (Fig. 4). The data presented in Fig. 4 indicates that the cardiac patients studied in this work have been suffering from intermediate hyperhomocysteinemia. Unprecedented clinical validation of our presented optical probe has also been performed by comparing the Hcy levels in a large number (sixty) of clinical samples. A clinically approved commercial immunoassay kit and current optical assay have been used to measure plasma tHcy levels in clinical samples. The results shown in Fig. S53 and Table S7 (ESI†) indicate that the Hcy level measured by the probe **1** compares reasonably well with the commercial kit. Thus, a simple and straightforward assay has been established in this work, which paves the way towards the possibility of the development of a miniature POCT kit for routine analysis and prognosis of various critical illnesses connected to HHcy in low resource settings.

In summary, we have reported herein a series of water soluble optical probes, which displayed a highly selective and interference-free turn-on fluorescence response towards homocysteine. EPR and UV-vis investigations provided evidence for the reduction-induced-emission-enhancement of the probes with Hcy. Validation of the presented optical assay has been performed by the traditional HPLC technique and reliability testing of **1** with regard to the clinically approved commercial immunoassay kit involving a large number of human plasma samples validates the simplicity and real-world application prospects of **1** as a novel molecular probe to measure the cardiac marker Hcy in patients' blood samples. Optical measurement of Hcy in human plasma samples using **1** and demonstration of its validation with sixty clinical samples is the first of its kind. The chemicals for preparing the probe and reagents required for the assay are inexpensive. Therefore, the present method reported herein demonstrates the feasibility for the development of a Hcy-selective diagnostic kit to be suitable for point-of-care testing.

This work is supported by the Govt. of India through the CSIR Grant no. MLP0047 and SERB (Grant no. CRG/2020/000577). SD and RRR acknowledge CSIR for their SRFs. The manuscript has CSIR-CSMCRI registration number 161/2021. Prior consent was obtained from human subjects.

Conflicts of interest

The authors declare no conflict of interest.

Notes and references

1 (*a*) G. E. Lonn, S. Yusuf, M. J. Arnold, P. Sheridan, J. Pogue, M. Micks, J. Probstfield, G. Fodor, C. Held and J. J. Genest, *N. Engl. J. Med.*, 2006, **354**, 1567–1577; (*b*) S. Seshadri, A. Beiser, J. Selhub, P. F. Jacques, I. H. Rosenberg, R. B. D'Agostino, P. W. F. Wilson and P. A. Wolf, *N. Engl. J. Med.*, 2002, **346**, 476–483; (*c*) H. Refsum and P. M. Ueland, *Annu. Rev. Med.*, 1998, **49**, 31–62; (*d*) M. Sibrian-Vazquez, J. O. Escobedo, S. Lim, G. K. Samoei and R. M. Strongin, *Proc. Natl. Acad. Sci. U. S. A.*, 2010, **107**, 551–554.

2 (*a*) W. Wang, J. O. Escobedo, C. M. Lawrence and R. M. Strongin, *J. Am. Chem. Soc.*, 2004, **126**, 3400–3401; (*b*) X. Yang, Y. Guo and R. M. Strongin, *Angew. Chem., Int. Ed.*, 2011, **50**, 10690–10693; (*c*) H. Peng, K. Wang, C. Dai, S. Williamson and B. Wang, *Chem. Commun.*, 2014, **50**, 13668–13671; (*d*) H. Y. Lee, Y. P. Choi, S. Kim, T. Yoon, Z. Guo, S. Lee, K. M. K. Swamy, G. Kim, J. Y. Lee, I. Shin and J. Yoon, *Chem. Commun.*, 2014, **50**, 6967–6969; (*e*) Z. Li, Z. R. Geng, C. Zhang, X. B. Wang and Z. L. Wang, *Biosens. Bioelectron.*, 2015, **72**, 1–9; (*f*) J. Wang, Y. Liu, M. Jiang, Y. Li, L. Xia and P. Wu, *Chem. Commun.*, 2018, **54**, 1004–1007; (*g*) J. O. Escobedo, W. Wang and R. M. Strongin, *Nat. Protoc.*, 2007, **1**, 2759–2762.

3 C. X. Yin, K. M. Xiong, F. J. Huo, J. C. Salamanca and R. M. Strongin, *Angew. Chem., Int. Ed.*, 2017, **56**, 13188–13198.

4 R. R. Nair, M. Raju, K. Jana, D. Mondal, E. Suresh, B. Ganguly and P. B. Chatterjee, *Chem. – Eur. J.*, 2018, **24**, 10721–10731.

5 D. Cao, Z. Liu, P. Verwilst, S. Koo, P. Jangjili, J. S. Kim and W. Lin, *Chem. Rev.*, 2019, **119**, 10403–10519.

6 D. Ray and P. K. Bharadwaj, *Inorg. Chem.*, 2018, **47**, 2252–2254.

7 H. Sung Jung, J. Hye Han, Y. Habata, C. Kang and J. Seung Kim, *Chem. Commun.*, 2011, **47**, 5142–5144.

8 U. Reddy, H. Agarwalla, N. Taye, S. Ghorai, S. Chattopadhyay and A. Das, *Chem. Commun.*, 2014, **50**, 9899–9902.

9 Q. Ma, X. Fang, J. Zhang, L. Zhu, X. Rao, Q. Lu, Z. Sun, H. Yu and Q. Zhang, *J. Mater. Chem. B*, 2020, **8**, 4039–4045.

10 D. Chao and Y. Zhang, *Sens. Actuators, B*, 2017, **245**, 146–155.

11 E. Faggi, R. Gavara, M. Bolte, L. Fajari, L. Juliá, L. Rodríguez and I. Alfonso, *Dalton Trans.*, 2015, **44**, 12700–12710.

12 E. Garribba and G. Micera, *J. Chem. Educ.*, 2006, **83**, 1229–1232.

13 X. F. Yang, Q. Huang, Y. Zhong, Z. Li, H. Li, M. Lowry, J. O. Escobedo and R. M. Strongin, *Chem. Sci.*, 2014, **5**, 2177–2183.

14 R. R. Nair, S. Debnath, S. Das, P. Wakchaure, B. Ganguly and P. B. Chatterjee, *ACS Appl. Bio Mater.*, 2019, **2**, 2374–2387.

15 E. Bald, E. Kaniowska, G. Chwatko and R. Glowacki, *Talanta*, 2000, **50**, 1233–1243.

Chemistry–A European Journal | Research Article
doi.org/10.1002/chem.202401255

PAPER-2

Chemistry Europe
European Chemical Societies Publishing

www.chemeurj.org

A Hydrogen Bonded Non-Porous Organic-Inorganic Framework for Measuring Cysteine in Blood Plasma and Endogenous Cancer Cell

Riya Ghosh,[a, b] Debjani Pradhan,[a, b] Snehasish Debnath,[a, b] Arushi Mansingh,[c] Narayana Nagesh,*[b, c] and Pabitra B. Chatterjee*[a, b]

An imbalance in cysteine (Cys) levels in the cells and plasma has been identified as the risk indicator for various human diseases. The structural similarity of cysteine with its congener homocysteine and glutathione offers challenges in its measurement. Herein, we report a hydrogen-bonded organic-inorganic framework of Cu(II) (HOIF) for the selective detection of cysteine over other biothiols. The non-fluorescent HOIF showed 12-fold green emission in the presence of cysteine. The monomeric unit of HOIF is stabilized via intermolecular hydrogen bonds, resulting in a non-porous network structure. Non-interference from homocysteine, glutathione, and other competitive bioanalytes revealed explicit affinity of HOIF for cysteine. Fluorimetric titration showed a wide working concentration window (650 nM–800 μM) for measuring cysteine in an aqueous medium. The mechanistic investigation involving HRMS, EPR, and UV-vis spectroscopic studies revealed the decomplexation of HOIF with Cys, resulting in a fluorescence turn-on response from the luminescent ligand. Validation using a commercial dye, "Cysteine Green", confirmed the prospect of HOIF for early diagnostic purposes. Utilizing the fluorescence turn-on property of HOIF in the presence of cysteine, we measured cysteine quantitatively in the blood plasma samples. Bio-imaging of endogenous cysteine in cancer cells indicated the ability of HOIF to monitor the intracellular cysteine.

Introduction

The biothiol cysteine (Cys) is associated with many enzymatic reactions and plays an active role in the cellular redox homeostasis.[1–3] The action of S-adenosylmethionine synthase on methionine (Met) in the presence of ATP initially results in the formation of the intermediate S-adenosylmethionine. This intermediate subsequently undergoes demethylation to produce S-adenosyl-L-homocysteine. Further, it converted to L-homocysteine (Hcy) in the presence of adenylhomocysteinase.[4] The reaction between serine (Ser) and homocysteine (Hcy), mediated by cystathionine β-synthase (CBS), produces L-cystathionine. In the presence of cystathionine γ-lyase (CTH), L-cystathionine is converted into cysteine (Cys) and (2Z)-amino-but-2-enolate as a by-product.[4] The normal levels of Cys in cells[5–7] and blood plasma[8–11] of humans are approximately 30–200 and > 250 μM, respectively. As the primary sulfide source in human metabolism, a typical concentration of Cys in cells is imperative for synthesizing various proteins.[6] Furthermore, as a precursor of the antioxidant glutathione, its level in human blood has been identified as the risk indicator for vascular diseases in the coronary, cerebral, and peripheral vessels.[9–12] Cys also plays a crucial role in determining how our body metabolizes energy, stores and breaks down fat, etc. Given the various roles of Cys in human biology, a drive to develop assays for measuring plasma Cys should facilitate the early assessment of health illnesses. The congeners of Cys, i.e., homocysteine (Hcy) and reduced glutathione (GSH), possess significant structural similarity (Scheme 1) to it. As a result, developing a Cys-specific fluorescent probe is a challenging task. Moreover, a high concentration of intracellular GSH (1–10 mM) provides further difficulty in measuring Cys.[13]

Over the last decade, substantial efforts have been made to develop analytical methods, including high-performance liquid chromatography (HPLC),[14] mass spectrometry,[15] potentiometry,[16] ELISA,[17] etc., for measuring cysteine. Even though some of these techniques are useful, most are tedious and costly. In contrast, the fluorescence technique has emerged as a fantastic tool for measuring Cys because of its simplicity, sensitivity, real-time detection ability, etc.[18–20] Fluorescent probes are highly effective molecular tools in analytical sensing and optical imaging due to their exceptional sensitivity, specificity, rapid response, and straightforward application.[21] These probes enable direct visualization and dynamic analysis of the location inside the living cells and the concentration of target biomolecules, offering valuable insights.[21]

In 2004, Kim et al. proposed an in-situ Cd(II) complex for the colorimetric detection of Cys.[22] Tae et al. developed a rhodamine-Au(I) probe for detecting Cys using the chemosensing ensemble method.[23] Zhao and his team reported a Ru(II)

[a] R. Ghosh, D. Pradhan, S. Debnath, P. B. Chatterjee
Analytical & Environmental Science Division and Centralized Instrument Facility, CSIR-CSMCRI, G. B. Marg, Bhavnagar, India
E-mail: pbchatterjee@csmcri.res.in

[b] R. Ghosh, D. Pradhan, S. Debnath, N. Nagesh, P. B. Chatterjee
Academy of Scientific and Innovative Research (AcSIR), 201002 Ghaziabad, India

[c] A. Mansingh, N. Nagesh
Medical Biotechnology Complex, CSIR-CCMB, ANNEXE II, Hyderabad, India
E-mail: nagesh@ccmb.res.in

Supporting information for this article is available on the WWW under https://doi.org/10.1002/chem.202401255

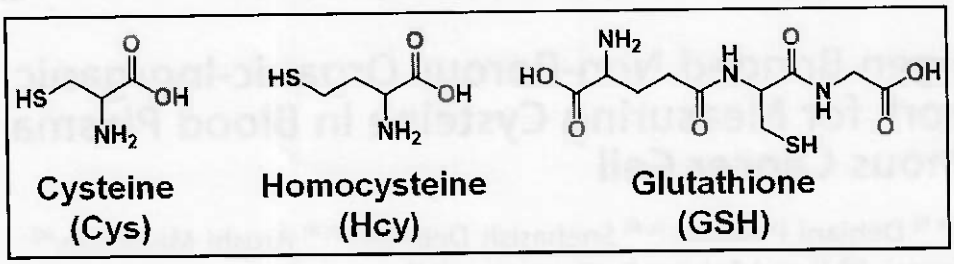

Scheme 1. Structures of cysteine, homocysteine, and reduced glutathione.

derived probe for detecting Cys via phosphorescence.[24] Wang and his group documented Cu(II) probe for monitoring Cys in plasma using dual colorimetric and fluorescence techniques.[25] Ma et al. have reported a long lifetime bearing Ir(III) complex, showing a turn-on luminescence response in the presence of Cys in live zebrafish.[26] Mayilmurugan et al. have developed a Cu(II) complex for the optical imaging of Cys in HeLa cells and macrophages.[27] Izake and his group proposed a paper-based Hg(II) derived probe for colorimetric detection of Cys.[28] Approximately nineteen inorganic Cu, Cd, Ru, Ir, and Hg complexes were reported for detecting Cys (Table S1) in organic-water solvent mixtures.[22–40] A few water-soluble probes are also documented (Table S1).[20,36,27,39] However, interference from competing biothiols was not performed in some cases.[22–23,29,26,28] Relatively high levels (approximately 250 μM) of Cys in blood plasma are found in a healthy individual, and its concentration further elevates in case of disease conditions (> 250 μM).[8–11] Thus, indicating the requirement of probes to be effective in directly measuring Cys at a relatively high concentration regime, typically > 250 μM. Table S1 discloses a compilation of the optical properties of cysteine selective inorganic compounds. A careful observation of the table reveals that the saturation limit of the Cys-selective inorganic complexes reported hitherto typically falls in the 5–200 μM region.[22,23,26–28,30,33–36,37,39,40] However, a few complexes work in the mM region.[24,32,38] The saturation limit for detecting Cys for most probes is around 200 μM or less.[22,23,25,27,30,33,34–36,37,40] Validation of the probes is indispensable to ascertain the applicability of the Cys-specific probes for early diagnostic purposes. Table S1 also reveals that this aspect has yet to be explored in the case of Cys-specific inorganic complexes.

This article reports the synthesis of a water-soluble (100% aqueous) hydrogen-bonded organic-inorganic (HOIF) framework of Cu(II) for measuring Cys directly in blood plasma and cells.[41,42] HOIF crystallizes in the monoclinic space group C2/c with eight molecular weight units accommodated in the unit cell. Single crystal analysis revealed that the molecular structure of the copper complex is extended via supramolecular hydrogen bonding with the amine group of thiosemicarbazide of two neutral complexes in N–H···N fashion. Water-soluble HOIF shows turn-on green emission in the presence of cysteine (Cys) without any interference from homocysteine, glutathione, and other competitive bio-analytes. The HOIF can detect cysteine at as low as 650 nM. Fluorimetric titration also showed that the HOIF can measure up to 800 μM cysteine, i.e., above the normal levels of Cys in cells and blood plasma. Fluorimetric measurement of cysteine by the HOIF has been validated using a commercial technique. HOIF can also function as a fluorescent dye to visualize the intracellular cysteine in cancer cells. EPR, HRMS, and UV-vis investigations proved the HOIF's decomplexation in the presence of cysteine. The quantitative measurement of cysteine in blood plasma by the HOIF offers a promising opportunity for healthcare diagnostics.

Results and Discussion

Syntheses and Characterization

3-Trimethylethylenediaminomethyl-5-bromosalicyldehyde is reacted with 4-methyl-3-thiosemicarbazide to obtain intramolecularly hydrogen-bonded zwitterion HL (Scheme 2). On reacting HL with Cu(II) acetate, the desired product Cu_2L_2 (i.e., HOIF) was

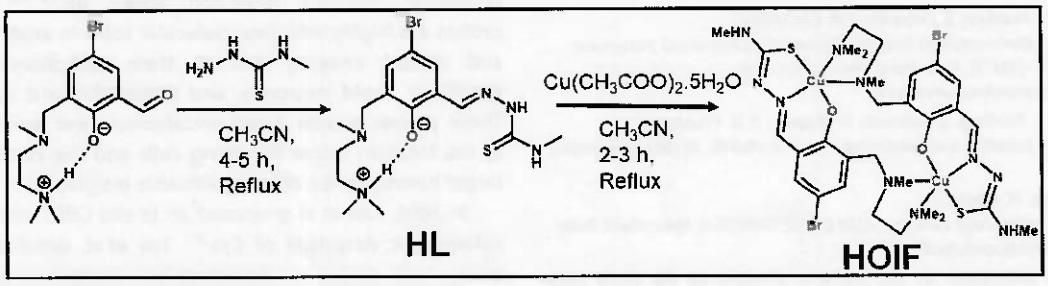

Scheme 2. Schematic representation of the syntheses of HL and HOIF.

formed (Scheme 2). As expected, the disappearance of the ν(O–H) band at 3245 cm^{-1} confirms the absence of the phenolic OH in HL, as observed earlier in the precursor zwitterion (Figure 1).[43] A stretch at 1032 cm^{-1} indicates the C=S bond in HL.[44,45] The formation of HL has been confirmed from the ^1H and ^{13}C NMR spectra (Figure 1). ^1H NMR of HL has been recorded at room temperature in $CDCl_3$, and data are summarized in the Experimental Section. A sharp singlet at δ 8.13 ppm confirms the presence of azomethyne H (Figure 1a). The existence of broad singlets at δ 8.88 and 7.47 ppm dictates the presence of two secondary amino H of the 4-methyl-3-thiosemicarbazide moiety of HL. The absence of any low field resonance beyond δ 8.88 ppm indicates the absence of thiol SH and phenolic OH groups in the ligand (Figure 1a). ^{13}C NMR spectrum (Figure 1b) of HL shows the presence of fourteen different types of carbons and, thus, confirms the ligand's formation. The existence of molecular ion peak in the positive mode of HRMS at m/z = 402.0950 indicates the formation of HL (Figure S1). Figure S1 reveals the presence of two peaks at m/z values 402.0950 and 404.0930 at 1:1 relative abundance, a characteristic of the two bromine isotopes.

Description of Crystal Structure

The ORTEP view and atom-labeling scheme of the organic-inorganic framework HOIF is shown in Figure 2. Diffraction quality crystal was obtained from an acetonitrile/water mixture. The complex crystallizes in a monoclinic space group C2/c and has eight molecular units per unit cell (Table 1). The Cu1 atom is coordinated with the imine nitrogen atom N1, sulfur atom S1, phenolic oxygen atom O1, and the amine nitrogen atoms N4′ and N5′. The asymmetric unit of HOIF comprises a deprotonated ligand, i.e., L^{2-} and one Cu^{2+} ion. The coordination environments around Cu is determined by the structural parameter τ, which is calculated from the equation $\tau = (\beta - \alpha)/60$ (where β and α are the two largest L–M-L angles). The τ value (= 0.076) suggests distorted square pyramidal geometry at the Cu(II) center with bond angles ranging from 81.32 to 102.85

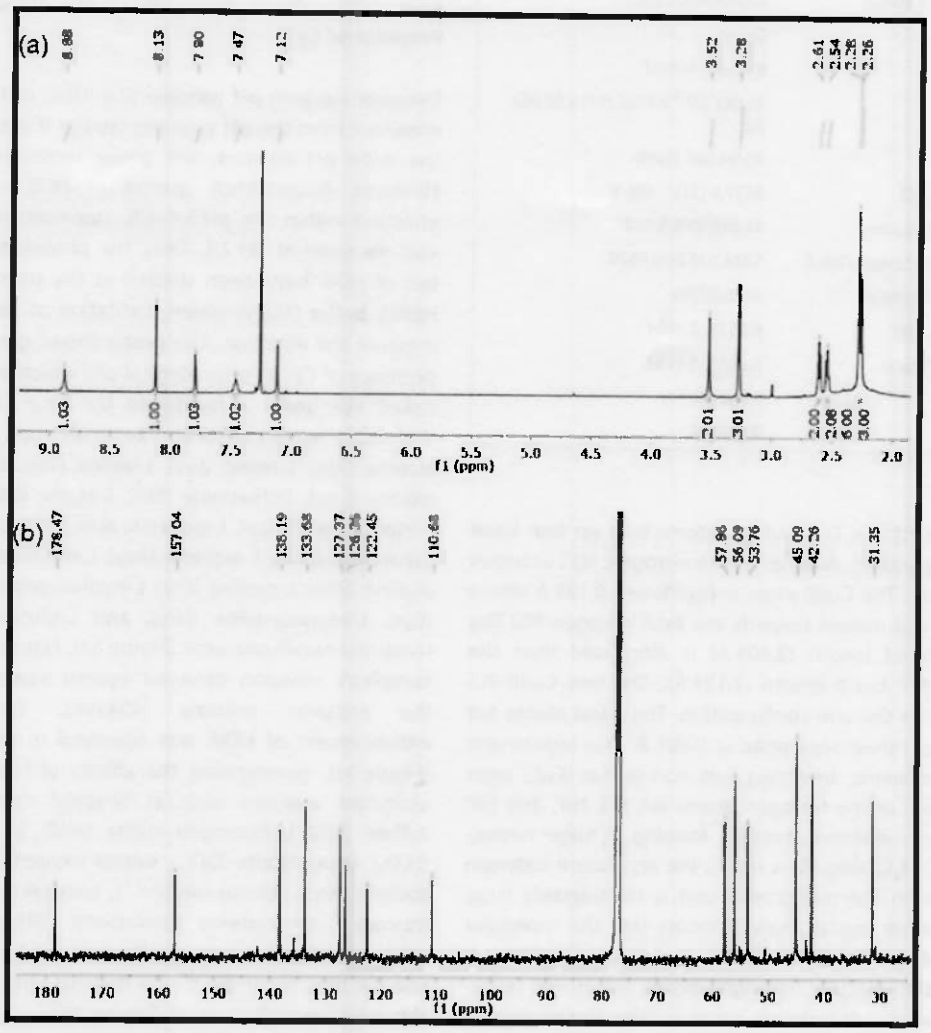

Figure 1. ^1H (a) and ^{13}C (b) NMR spectra of HL in $CDCl_3$.

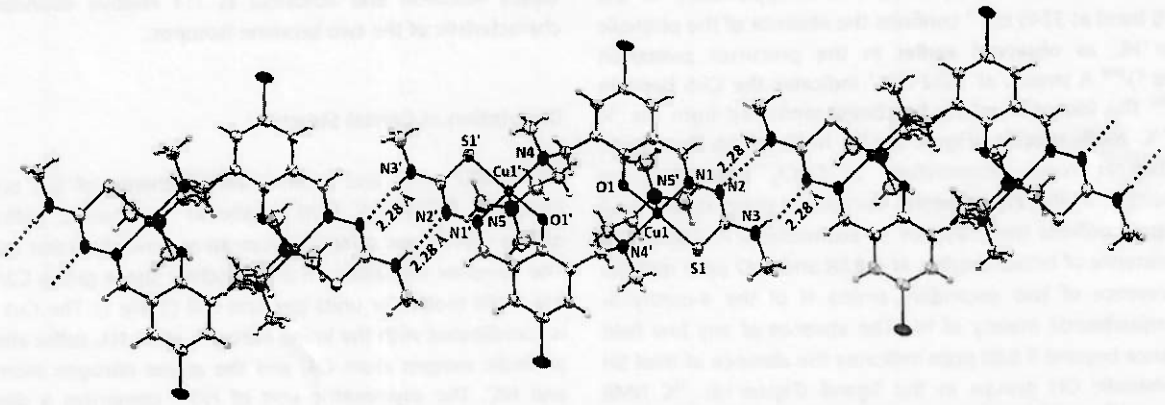

Figure 2. Crystal structure and atom labelling scheme for HOIF. Hydrogen bonding interactions between the monomeric units of HOIF are shown above.

Table 1. Crystallographic data of HOIF.

Parameters	HOIF (Cu2L2)
Molecular Formula/Formula Weight	$C_{15}h_{22}n_5osbrcu$/463.88
Crystal System/Space Group	Monoclinic/C2/C
Crystal Color	Green
Crystal size/mm^3	0.14×0.11×0.07
a (Å)/b (Å)/c (Å)	25.061 (4) / 7.1766 (11) / 20.262 (4)
α (°)/β (°)/γ (°)	90/94.609 (8)/90
V(Å^3)/Density (g/cm^3)/Z	3632.5 (11)/1.696/8
$2\theta_{max}$ [deg]/Temp (K)/μ, mm^{-1}	51.838/298/3.530
Reflections Collected/Unique/R(int)	58242/3525/0.0579
Data/Restraints/Parameters	3525/0/240
R1(F_0), *wR2*(F_0) ($I \geq 2\sigma(I)$)	0.0522, 0.1484
R1(F_0^2), *wR2*(F_0^2) (all data)	0.0633, 0.1193
F(000)/GOF on F^2	1880.0/1.147
CCDC No.	2339054

(Table S2).[43] The N1, S1, O1, and N4′ atoms take up four basal positions of the pyramid. Another amine nitrogen, N5′, occupies the apical position. The Cu(II) atom is positioned 0.195 Å above the basal plane and moved towards the axial nitrogen N5. The axial Cu1–N5′ bond length (2.408 Å) is elongated than the equatorial Cu1–N4′ bond length (2.131 Å). The two Cu(II)–N5 apical bonds are in the anti-configuration. The basal planes are not co-planar, and their separation is 0.891 Å. The monomeric unit is centrosymmetric, involving two non-planar [CuL] units connected by four amine nitrogen atoms N4, N5, N4′, and N5′ from the hanging diamine moieties forming a huge twelve-membered $Cu_2O_2N_2C_6$ ring. As a result, the separation between two Cu(II) atoms in the monomeric unit is considerably large (6.452 Å). The single crystal analysis shows that the molecular arrangement of the Cu(II) complex in crystal packing is stabilized via intermolecular hydrogen bonds N2–H···N3, resulting in a non-porous 1 D network structure. The intermolecular H bonding distance and N–H···N angels between two adjacent monomer units is about 2.28 Å and 174°, respectively, indicating the presence of intermolecular H bonding.[46]

Excited State Photophysical Properties of HOIF in the Presence of Cys

Dynamic working pH window (2.6–10.6) of the HOIF has been observed from the pH profiling studies (Figure S2). Throughout the wide pH window, the probe remained non-fluorescent. However, fluorescence spectra of HOIF with Cys showed emission within the pH 6.4–8.6. However, maximum emission was observed at pH 7.4. Thus, the photoluminescence properties of HOIF have been studied at the physiological pH using HEPES buffer (100% water). Excitation at 380 nm was used to measure the emission. The probe shows green emission in the presence of Cys at physiological pH, which is observable by the naked eye under a hand-held UV lamp (365 nm, Figure S3). With other amino acids and biothiols such as glycine (Gly), L-alanine (Ala), L-lysine (Lys), L-valine (Val), L-isoleucine (Ile), L-leucine (Leu), L-threonine (Thr), L-serine (Ser), L-histidine (His), L-aspartic acid (Asp), L-glutamic acid (Glu), L-glutamine (Gln), L-asparagine (Asn), L-arginine (Arg), L-methionine (Met), L-phenyl alanine (Phe), L-proline (Pro), L-hydroxyproline (Hyp), L-cysteine (Cys), L-homocysteine (Hcy), and L-glutathione (GSH), HOIF remained non-fluorescent (Figure S3). Figure 3a shows the Cu(II) complex's emission behavior against various amino acids. At the emission maxima (494 nm), 12-fold fluorescence enhancement of HOIF was observed in the presence of Cys (Figure 3a). Investigating the affinity of HOIF with various cell abundant analytes such as N-acetyl cysteine, sulfide (S^{2-}), sulfate (SO_4^{2-}), hydrogen sulfite (HSO_3^-), hydrogen peroxide (H_2O_2), hypochlorite (OCl^-), singlet oxygen ($^1O_2$), calcium (Ca^{2+}), sodium (Na^+), ferrous ion (Fe^{2+}), adenosine triphosphate (ATP), glucose, homocysteine thiolactone, dithioerythritol, ascorbic acid, and human serum albumin (HSA) reveals (Figure 3b) specific binding of the probe towards Cys. This study indicates the selective detection of Cys by HOIF among various amino acids, biothiols, and other competing analytes in biofluids. To ensure the non-interference from other challenging analytes,

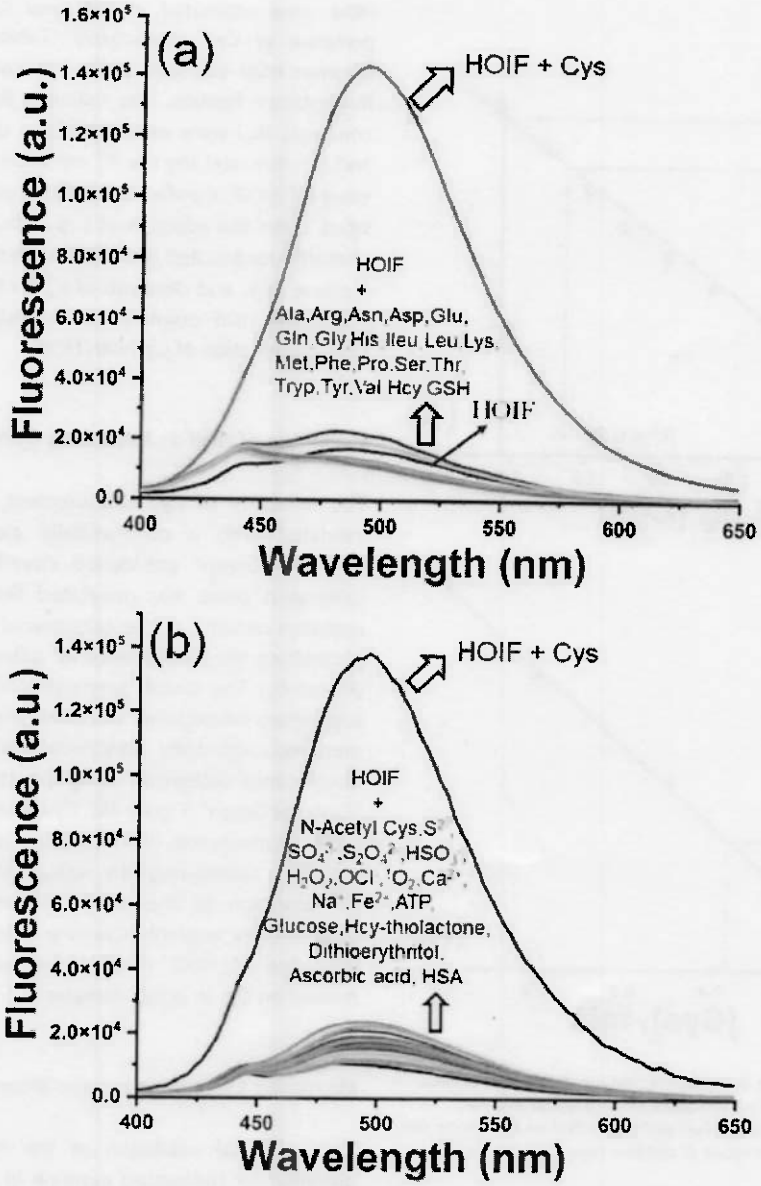

Figure 3. Fluorimetric responses of HOIF (20 μM) with various solutions (125 μM) of (a) amino acids and (b) other competing analytes in aqueous HEPES solution (10 mM) at physiological pH.

the fluorescence of HOIF was monitored in the presence of the equivalent amount of each analyte and cysteine (Figure S4). Figure S4 explains the interference-free affinity of HOIF for Cys in the presence of other amino acids/biothiols (Figure S4a) and other bio-analytes (Figure S4b). We also performed the interference study of HOIF in the presence of 50 μM Hcy and 1 mM GSH (Figure S5) and found that the probe can detect Cys in the presence of Hcy and GSH.

The time-responsive behavior of the probe with Cys showed maximum emission of HOIF after 10 min incubation with Cys (Figure S6). Thus, the steady-state luminescence spectra of HOIF were measured after 10 min incubation of each analyte. Next, the concentration-dependent fluorescence experiments were performed, and calibration curves were generated (Figure S7). Using the titration data points, a non-linear calibration curve has been developed by plotting the fluorescence vs. concentration ratio of the analytes and HOIF (Figure S8). The calibration plot was used to calculate the binding constant between HOIF and Cys.[47,48] The association constant was $6.8\times10^4\ M^{-1}$ (Figure S8). For the estimation of the limit of detection (LOD), a plot of $(F-F_0)/(F_\infty-F_0)$ against log[Cys] has been generated, as shown in Figure 4a.[47] Here, F_0 and F are the emission intensities of HOIF without and with the addition of a specific concentration of Cys, respectively. Where F_∞ is the intensity of HOIF in the presence of the highest concentration of Cys used in the titration. The calculated LOD was 650 nM, far below the normal

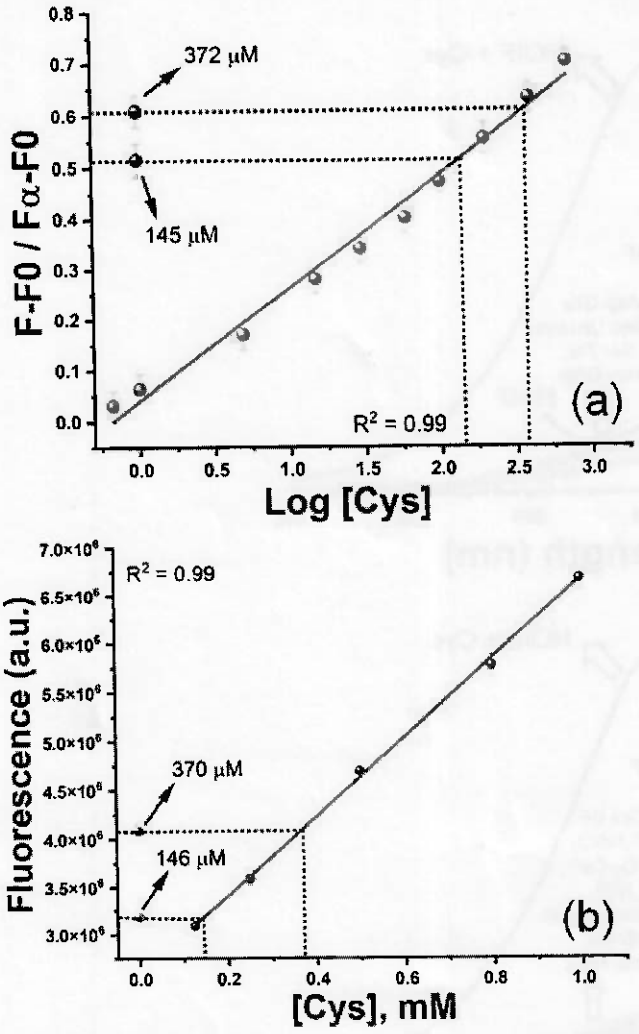

Figure 4. (a) Linear fitting of the fluorescence titration data points against variable concentrations of cysteine in aqueous HEPES buffer solution (10 mM) at physiological pH. (b) Standard plot generated via measuring the fluorescence of various concentrations of cysteine using standard dye "Cysteine Green".

range of Cys (250 μM) present in blood plasma and cells (Figure 4a). The stability of the probe was evaluated using UV-vis and fluorescence techniques, and the results are shown in Figure S9. UV-vis (Figure S9a) and fluorescence (Figure S9b) data of 20 μM aqueous HEPES solution (pH 7.4) of HOIF in different time intervals were recorded. Results indicate that the probe remains stable for an extended period. Furthermore, temperature-dependent fluorescence experiments of HOIF were also performed in the HORIBA CANADA Fluorolog-QM™ instrument. Results shown in Figure S10 demonstrate that HOIF is stable at a wide temperature range, specifically from 10–70 °C.

To investigate the excited state behavior of HOIF, time-correlated single-photon counting (TCSPC) experiments were performed (Figure S11). The excitation and emission wavelengths were 375 and 494 nm, respectively. Single exponential fitting conveyed the best decay profile. The quantum yields of HOIF were estimated at 0.03 and 0.35 in the absence and presence of Cys, respectively (Table 2). Adding Cys to the aqueous HOIF solution resulted in insignificant changes in the fluorescence lifetime. The radiative (k_r) and non-radiative rate constants (k_{nr}) were estimated from the equations $k_r + k_{nr} = \tau^{-1}$ and $k_r = \Phi_f/\tau$, and the results are shown in Table 2.[47] The low k_r value of HOIF signifies its non-emissive behavior. A high k_{nr} value upon the addition of Cys indicates the existence of the photoinducedexcited electron transfer (PET) process.[47] A drastic increase of k_r and decrease of k_{nr} on the addition of Cys to the solution of HOIF points to the formation of a new species due to the interaction of Cys with HOIF.

Validation of HOIF in Measuring Cysteine

The reliability of Cys measurement by HOIF has next been validated with a commercially available fluorescence dye "Cysteine Green" pre-loaded cuvette kit. In brief, a linear calibration curve was generated first using the fluorescence emission maxima of the commercial dye at 525 nm and then plottedting the fluorescence vs. different concentrations of Cys (Figure 4b). The sample preparation method is described in the supporting information. Next, two unknown Cys solutions were prepared, and their concentrations were measured by the fluorescence technique using the standard calibration plot of "Cysteine Green" (Figure 4b). Cysteine Green and HOIF (Figure 4, Table 3) measured the concentrations of the unknown Cys solutions. Comparing the values in Table 3 reveals a good corroboration of the results obtained from HOIF with the commercially available Cysteine Green kit. Thus, the analytical validation of HOIF showed the reliability of the probe for measuring Cys in actual samples.

Measuring Cysteine in Human Blood Plasma Using HOIF

The analytical validation of the HOIF showed the probe's potential for measuring cysteine in actual samples. Therefore,

Table 2. Quantum yields (Φ_f), lifetimes (τ), radiative/non-radiative rate constants (k_r and k_{nr}), and χ^2 (fitting parameter) values.

Sample	τ	ϕ	k_r	k_{nr}	χ^2
HOIF	0.51	0.03	0.05	0.67	0.974
HOIF + Cys	0.51	0.35	0.67	0.12	0.980

Table 3. Measurements of cysteine in blood plasma using HOIF and Cysteine Green dye via fluorescence method.

Sample ID	Cys Concentration by HOIF	Cys Concentration by Cysteine Green
Sample - 1	145 μM	146 μM
Sample - 2	372 μM	370 μM

we next tested HOIF in the blood samples. Different Cys samples were prepared by spiking different concentrations of Cys to the plasma samples, and the fluorescence of the mixtures was recorded using a 20 μM aqueous solution of HOIF. A linear calibration curve is made, as shown in Figure 5. With an increase in the concentrations of Cys, the fluorescence of HOIF rises linearly. We then measured the fluorescence of two unknown plasma samples (Cys-spiked), and the concentrations 112 and 229 μM were calculated from the linear calibration plot (Figure 5). Next, we added 15 μM of Cys solutions to each unknown sample and recorded fluorescence in the presence of HOIF. The concentrations of the latter two solutions were found at 125 and 246 μM, respectively (Figure 5). The result shown in Figure 5 indicates that HOIF can develop a miniature POCT kit for routine analysis of Cys in plasma samples.

In-Vitro Toxicity Studies

In-vitro cytotoxicity of HOIF was evaluated using a lung cancer cell line (A549) and a normal (non-cancerous) cell line (HFF). Cytotoxicity of the probe was determined using MTT (3-(4,5-dimethylthiazol-2-yl)-2,5-diphenyltetrazolium bromide) assay[49,50] and their half maximum inhibitory potential values, i.e., IC_{50} are shown in Figure S12. Results shown in Figure S12 indicate that the IC_{50} value of HOIF in the A549 cell line is comparatively close to the value obtained in the HFF cell line.

Microscopic Studies

To further evaluate the ability of HOIF to monitor Cys in living cells, we incubated the probe in the A549 cells for 30 min, and the fluorescence was observed under a green channel (Figure 6a). Results shown in Figure 6a indicate the presence of intracellular Cys in A549 cells directly without adding extra Cys to enhancinge the fluorescence intensity, which is helpful in the actual intracellular cysteine measurement. Further, some cells were pre-treated with 500 μM N-ethylmaleimide (NEM, an intracellular thiol scavenger) and then incubated with HOIF for 30 min.[5] No fluorescence was observed in the green channel (Figure 6b). Moreover, cells pre-treated with 500 μM NEM, when treated further with HOIF for another 30 min and then incubated with 50 μM Cys for an additional 30 min, showed green fluorescence. Presumably, the interaction of the probe with the excess cysteine supplied to the system resulted in fluorescence seen in the green channel (Figure 6c). Together, these observations indicated that HOIF could detect Cys in living cells.

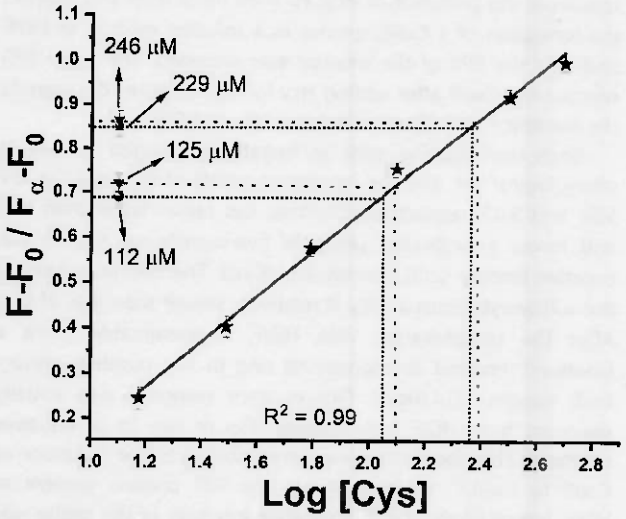

Figure 5. Linear fitting plot generated by measuring fluorescence at 494 nm of various concentrations of cysteine with HOIF (20 μM) in blood plasma. Four unknown solutions were also measured in this study.

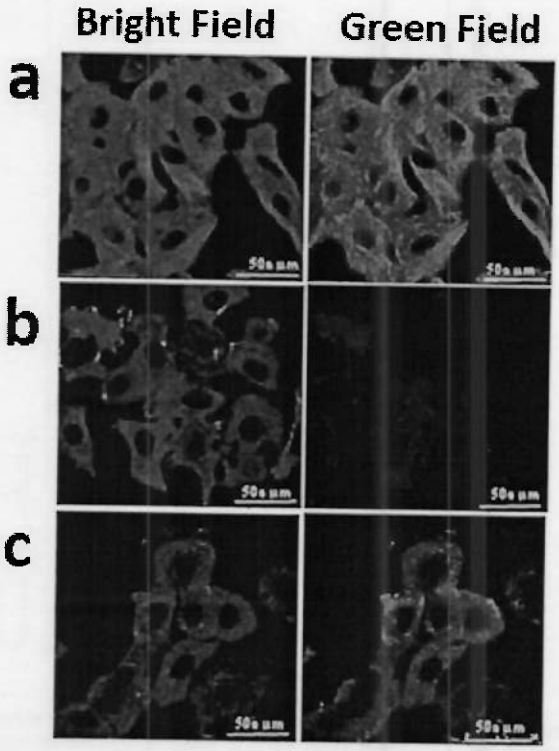

Figure 6. (a) Confocal fluorescence images of A549 cells. The images of A549 cells after incubating with HOIF (20 μM) for 30 min. (b) Images of A549 cells pre-treated with 1 mM NEM. (c) Images of NEM-treated A549 cells after 30 min additional incubation with 50 μM Cys. Excited at 380 nm, and emission was noticed at 494 nm. The scale bar is at 50 μm.

Mechanistic Investigation

To investigate the mechanism of interaction between HOIF and Cys, UV-vis spectra 20 μM HOIF, 125 μM Cys, and a mixture of 125 μM cysteine and 20 μM HOIF (Figure 7a) were recorded. HOIF and HL showed UV-vis maxima at 396 and 380 nm, respectively. A blue shift of the UV-vis peak of HOIF was observed after adding five equivalents of cysteine into its solution,. They presumably confirming the regeneration of HL from HOIF by cysteine. HRMS of HOIF after 10 min incubation

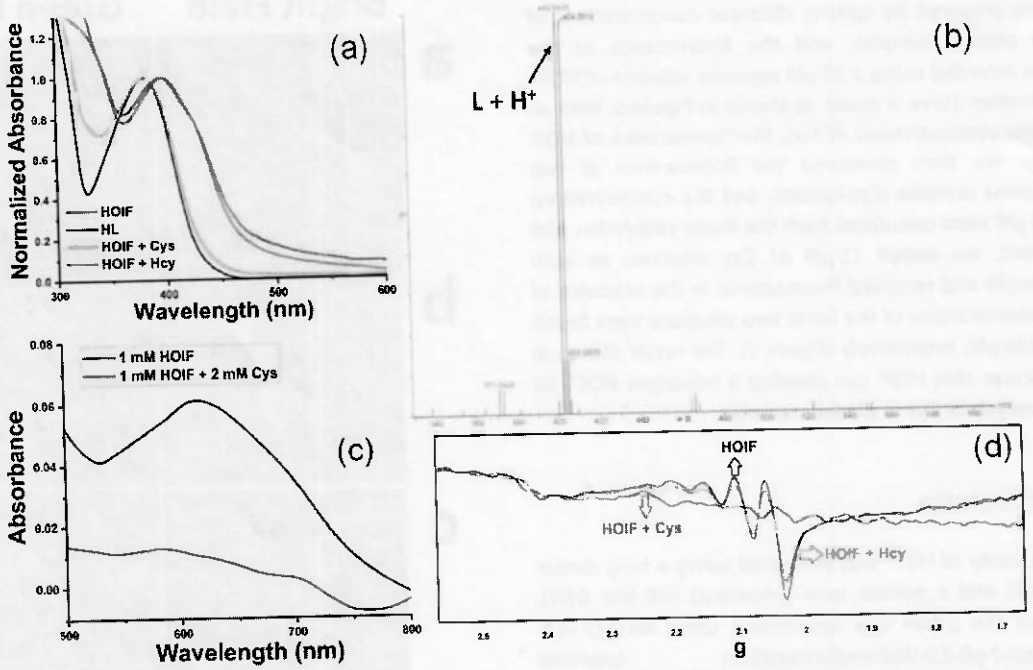

Figure 7. (a) UV-Vis spectra of HL (20 μM), HOIF (20 μM), a mixture of cysteine/homocysteine and HOIF. (b) HRMS profile of HOIF in the presence of cysteine. (c) Visible region absorption spectra of HOIF in the absence and presence of cysteine. (d) EPR spectra of HOIF without and with cysteine and homocysteine.

with Cys was recorded, and the molecular ion peak with m/z (L $+H^+$) at 402.0933 and 404.0918 (Figure 7b) was observed. The regeneration of the HRMS peaks of ligand implies the demetalation of HOIF in the presence of Cys (Figure 7b).[36,47] MS and UV-vis spectroscopic experiments indicate ligand displacement from HOIF on interaction with Cys. Literature documented that cysteine reduces Cu(II) to Cu(I).[32] The strong binding ability of cysteine and copper resulted in the removal of copper from the complex and the regeneration of the ligand.[36,51] HOIF showed a d-d band at 610 nm with a molar extinction coefficient of 60 $Lmol^{-1}cm^{-1}$, which is typical for the Cu^{2-} complex (d^9 system).[47] However, the complete disappearance of the d-d transition band with the addition of Cys indicates the formation of Cu(I) species (d^{10} system, Figure 7c).

The retention of the square pyramidal geometry of Cu(II) in aqueous solution has been evident from the EPR data. An aqueous solution of HOIF showed a four-line rhombic EPR spectrum.[35] Figure 7d reveals nuclear hyperfine splitting, which can be resolved in the parallel region with $g_{||} = 2.14$ with $A_{||} = 79\times10^{-4}\ cm^{-1}$. EPR feature of the other g tensors provided the highest g component $g_{\perp} = 2.04$ along with the hyperfine coupling value $A_{\perp} = 80\times10^{-4}\ cm^{-1}$. Thus, in the aqueous solution, the observed g values of HOIF can be arranged in the order of $g_{||} > g_{\perp} > 2.0023$, indicative of a typical EPR spectrum of a square pyramidal Cu(II) center.[35] Moreover, the $A_{||}$ value of $79\times10^{-4}\ cm^{-1}$ implies that HOIF adopts a distorted square pyramidal geometry ($A_{||}$ values typically range from 154 to $162\times10^{-4}\ cm^{-1}$ for ideal square-based geometries).[35,52] However, the EPR silent spectrum after the addition of Cys to the solution of HOIF indicates the formation of Cu(I) species (Figure 7d). MS, EPR, and UV-vis spectroscopic investigations altogether confirmed the reduction of Cu^{2+} to Cu^{+} by Cys, followed by the regeneration of the ligand, which is responsible for the observed fluorescence of HOIF in the presence of Cys. Interestingly, UV-vis spectroscopic studies of HOIF with homocysteine showed a d-d band at 595 nm with a molar extinction coefficient of 54 $Lmol^{-1}cm^{-1}$ (Figure S13). Moreover, the UV spectrum of HOIF in the presence of Hcy remained unchanged (Figure 7a). Thus indicating the formation of a ternary Cu(II) species in the presence of Hcy. To shed more light and support the formation of a Cu(II) species in a solution mixture of HOIF and Hcy, the EPR of the mixture was recorded. The 4-line EPR spectrum of Cu(II) after adding Hcy to HOIF (Figure 7d) suggests the existence of Cu(II) when adding Hcy to HOIF.

Both Hcy and Cys exist as negatively charged species at physiological pH, and the isoelectric points of Hcy and Cys are 5.65 and 5.02, respectively.[53] Thus, Cys reacts faster than Hcy and forms a kinetically unstable five-membered ring in the putative ternary Cu(I) species [CuL(Cys)]. The deprotonation of the sulfhydryl group of Hcy is relatively slower than that of Cys. After the complexation with HOIF, it presumably forms a kinetically favored six-membered ring in the putative ternary Cu(I) species [CuL(Hcy)]. Fluorescence response was initially observed from HOIF upon adding Cys or Hcy to its aqueous solutions. This observation can be attributed to the reduction of Cu(II) to Cu(I),[54] which disrupts the PET process present in HOIF. Interestingly, the fluorescence intensity of the probe was dramatically quenched for Hcy after 2 min incubation, indicating quick oxidation of Cu(I) to Cu(II) by the dissolved oxygen in the medium. Because of the decomplexation of the unstable

ternary species of Cu(I) with Cys, the ligand L is regenerated, which is responsible for the persistent fluorescence of HOIF upon incubation with Cys for 5 min or more.

Conclusions

We have reported a water-soluble hydrogen-bonded organic-inorganic framework (HOIF) of Cu(II) from substituted 3-trimethylethylenediaminomethyl-5-bromosalicyldehyde (HL) and copper(II) acetate. The monomeric unit of HOIF contains two non-planar [CuL] units that form a twelve-membered $Cu_2O_2N_2C_6$ ring. The intermolecular hydrogen bonding of the amine group of 4-methyl-3-thiosemicarbazide of two adjacent monomers in N–H···N fashion resulting in a non-porous 1 D network structure of HOIF. The probe HOIF displayed specific turn-on (fluorescence) responses with Cys compared to other structurally and functionally competing analytes, Hcy and GSH. Fluorimetric titration showed that the HOIF can measure up to 800 μM 650 nM cysteine, i.e., above the normal levels of Cys in cells and blood plasma. Investigations based on HRMS, EPR, and UV-vis provided evidence for the ligand displacement from HOIF in the presence of Cys. Validation with a commercially available dye attests to the real-world usefulness of HOIF. The probe was also utilized as a fluorescent dye to visualize the intracellular cysteine in cancer cells. Moreover, quantitative measurement of cysteine in blood plasma provides a promising opportunity for healthcare diagnostics. We expect that HOIF may be further explored in biomedical applications.

Experimental Section

Synthesis of HL

3-Trimethylethylenediaminomethyl-5-bromosalicyldehyde (315 mg, 1 mmol) and 4-methyl-3-thiosemicarbazide (105 mg, 1 mmol) were dissolved in acetonitrile (15 mL) solvent and refluxed under stirring for 4–5 h. Yellow precipitates of HL were formed after the reaction. The precipitates were filtered and washed thoroughly with cold acetonitrile. Recrystallization from the methanol solution of HL yielded crystalline HL. Yield: 72%. M.P: 165 °C. Selected IR bands (cm^{-1}): 3360, 2788, 1592, 1538, 1432, 1362, 1322, 1256, 1032, 917, 872, 811, and 762. ^1H NMR ($CDCl_3$, 600 MHz, δ ppm) 11.40 (s, 1H, NH), 8.40 (s, 1H, azomethyne H), 8.14 (s, 2H, NH_2), 8.05 (s, 1H, ArH), 7.15 (s, 1H, ArH), 3.63 (s, 2H, CH_2), 2.61 (m, 2H, CH_2), 2.58 (m, 2H, CH_2), 2.26 (s, 6H), and 2.22 (s, 3H). ^{13}C NMR ($CDCl_3$, 150 MHz, δ ppm) = 178.47, 157.04, 138.19, 133.68, 127.37, 126.36, 122.45, 110.68, 57.86, 56.09, 53.76, 45.09, 42.26, and 31.35. HRMS (m/z) [L + H^+] calcd: 402.0963. Found: 402.0950. Anal. Calcd (%) for $C_{15}H_{24}N_5OSBr$: C, 44.78; H, 6.01; N, 17.41; S, 7.97. Found: C, 44.75; H, 5.98; N, 17.36, S, 8.02. UV-vis (CH_2Cl_2) [λ_{max}, nm; ε, $Lmol^{-1}cm^{-1}$]: 348 (29101), 315 (24067), and 305 (25240).

Synthesis of $[Cu_2L_2]$ (HOIF)

To a 15 mL stirred acetonitrile solution of HL (402 mg, 1 mmol), solid Cu(II) acetate (182 mg, 1 mmol) was added and refluxed under stirring for 2–3 h. Green precipitates formed after the reaction. The precipitates were filtered and recrystallized from hot methanol. Yield: 68%. Selected IR bands (cm^{-1}): 3454, 3277, 1588, 1502, 1424, 1406, 1311, 1212, 1158, 1013, 954, 881, 791, 746, and 695. Anal. Calcd (%) for $C_{30}H_{44}N_{10}O_2S_2Br_2Cu_2$: C, 38.84; H, 4.78; N, 15.10; S, 6.91. Found: C, 38.85, H, 4.83; N, 15.06; S, 6.94. UV-vis (water) [λ_{max}, nm; ε, $Lmol^{-1}cm^{-1}$]: 384 (3803) and 317 (5510).

MTT Data

The MTT [3-(4,5-dimethylthiazol-2-yl)-2,5-diphenyltetrazolium bromide] assays[49,50] were performed using cancerous and normal cell lines. A549 (Lung cancer) and HFF cells (fibroblast cells that were isolated from the foreskin) were procured from American-type culture collection (ATCC) and sub-cultured. The cell lines were initially grown in 25 cm^2 bottle canted neck flasks (Corning) with Dulbecco modified essential F12 (DMEM–F12) medium supplemented with 20% fetal bovine serum (FBS), 3 mM L-glutamine, along with the addition of antibiotic solution consist of penicillin 500 U/mL and streptomycin 500 μg/mL to protect the cell lines from bacterial infections and the cells were maintained in a humidified atmosphere of 5% CO_2 at 37 °C. The cells were passaged enzymatically with 0.25% trypsin in 1 mM EDTA and subcultured on 75 cm^2 plastic flasks at 2.3×10^4 cells/cm^2 density. The culture medium was replaced every two days. Cell confluence (80%) was confirmed by microscopic observance. Different concentrations of HOIF were added to the medium and incubated for 48 h at 37° C. Blank (i.e., without adding HOIF) was considered a positive control. Then 10 μL of 5 mg/mL MTT was added to each well, and the cultures were further incubated for an additional 4 h until purple formazan crystals were formed. The crystals were dissolved in DMSO, and the absorbance of each well was recorded at 570 nm using a BioTek Synergy H1 multimode microplate reader. Three replicate wells were used for each concentration, and each assay was measured three times, after which the cell viability was calculated.

Microscopy Data

A549 cells were treated with 20 μM HOIF for 30 min. After a thorough wash with PBS buffer (2–3 times), the fluorescence of the cells was checked directly for the presence of inherent cysteine in the cell. HOIF was dissolved in 10 mM HEPES buffer at pH 7.4. Further, the cells were treated with 1 mM NEM, and then a solution of 20 μM HOIF was added to the mixture and incubated for 30 min at 37 °C. Finally, 50 μM cysteine was added to the earlier mixture and incubated for 30 min. The photographs of the cells were taken under the fluorescence microscope.

Supporting Information Summary

The authors have cited additional references within the Supporting Information.[22–40,43,45]

Acknowledgements

This work is supported by the funding agency SERB, Govt. of India (Grant no. CRG/2020/000577). CSMCRI pris number 39/2024 has been assigned to this manuscript. We acknowledge the analytical support of AESD&CIF of CSIR-CSMCRI.

Conflict of Interests

The authors declare no conflict of interest.

Data Availability Statement

The data that support the findings of this study are available on request from the corresponding author. The data are not publicly available due to privacy or ethical restrictions.

Keywords: Analytical validation · Bio-imaging · Cysteine · Hydrogen-bonded organic inorganic framework · Testing human blood plasma

[1] B. D. Paul, J. I. Sbodio, S. H. Snyder, *Trends in Pharmacol. Sci.* **2018**, *39*, 513–524.
[2] C. E. Paulsen, K. S. Carroll, *Chem. Rev.* **2013**, *113*, 4633–4679.
[3] Y. Yu, H. Xu, W. Zhang, B. Wang, Y. Jiang, *Talanta* **2018**, *176*, 151–155.
[4] A. P. A. Dos Santos, J. K. Da Silva, J. M. Neri, A. C. O. Neves, D. F. De Lima, F. G. Menezes, *Org. Biomol. Chem.* **2020**, *18*, 9398–9427.
[5] B. Yang, J. Xu, Z.-H. Yuan, D.-J. Zheng, Z.-X. He, Q.-C. Jiao, H.-L. Zhu, *Talanta* **2018**, *189*, 629–635.
[6] Y. Yue, F. Huo, P. Ning, Y. Zhang, J. Chao, X. Meng, C. Yin, *J. Am. Chem. Soc.* **2017**, *139*, 3181–3185.
[7] N. Wang, M. Chen, J. Gao, X. Ji, J. He, J. Zhang, W. Zhao, *Talanta* **2019**, *195*, 281–289.
[8] A. Lima, R. Ferin, A. Fontes, E. Santos, D. Martins, J. Baptista, M. L. Pavão, *Nutr. Metab. Cardiovasc. Dis.* **2020**, *30*, 1281–1288.
[9] N. Jacob, E. Bruckert, P. Giral, M. J. Foglietti, G. Turpin, *Atherosclerosis* **1999**, *146*, 53–59.
[10] Y. Özkan, E. Özkan, B. Şimşek, *Int. J. Cardiol.* **2002**, *82*, 269–277.
[11] A. Valente, M. R. Bronze, M. Bicho, R. Duarte, H. S. Costa, *J. Sep. Sci.* **2012**, *35*, 3427–3433.
[12] B. J. Mills, M. M. Weiss, C. A. Lang, M. C. Liu, C. Ziegler, *J. Lab. Clin. Med.* **2000**, *135*, 396–401.
[13] T. Nagendraraj, S. V. Priya, J. Annaraj, S. Sagadevan, *Coord. Chem. Rev.* **2023**, *495*, 215368–215396.
[14] R. Głowacki, J. Stachniuk, K. Borowczyk, *Acta Chromatogr.* **2016**, *28*, 333–346.
[15] M. Rafii, R. Elango, G. Courtney-Martin, J. D. House, L. Fisher, P. B. Pencharz, *Anal. Biochem.* **2007**, *371*, 71–81.
[16] D. Jia, F. Li, L. Sheng, Q. Ren, S. Dong, S. Xu, Y. Mu, Y. Miao, *Electrochem. Commun.* **2011**, *13*, 1119–1122.
[17] H. Han, F. Wang, J. Chen, X. Li, G. Fu, J. Zhou, D. Zhou, W. Wu, H. Chen, *J. Alzheimer's Dis.* **2021**, *82*, 527–540.
[18] G. Liu, D. Liu, X. Han, X. Sheng, Z. Xu, S. H. Liu, L. Zeng, J. Yin, *Talanta* **2017**, *170*, 406–412.
[19] Q. Wang, H. Wang, J. Huang, N. Li, Y. Gu, P. Wang, *Sens. Actuators B: Chem.* **2017**, *253*, 400–406.
[20] H. Sheng, Y. Hu, Y. Zhou, S. Fan, Y. Cao, X. Zhao, W. Yang, *Dyes Pigm.* **2019**, *160*, 48–57.
[21] H. Zhu, J. Fan, J. Du, X. Peng, *Acc. Chem. Res.* **2016**, *49*, 2115–2126.
[22] M. S. Han, D. H. Kim, *Tetrahedron* **2004**, *60*, 11251–11257.
[23] Y. K. Yang, S. Shim, J. Tae, *Chem. Commun.* **2010**, *46*, 7766–7768.
[24] S. Ji, H. Guo, X. Yuan, X. Li, H. Ding, P. Gao, C. Zhao, W. Wu, W. Wu, J. Zhao, *Org. Lett.* **2010**, *12*, 2876–2879.
[25] W. Hao, A. McBride, S. McBride, J. P. Gao, Z. Y. Wang, *J. Mater. Chem.* **2011**, *21*, 1040–1048.
[26] Z. Mao, M. Wang, J. Liu, L.-J. Liu, S. M.-Y. Lee, C.-H. Leung, D.-L. Ma, *Chem. Commun.* **2016**, *52*, 4450–4453.
[27] S. Priyanga, T. Khamrang, M. Velusamy, S. Karthi, B. Ashokkumar, R. Mayilmurugan, *Dalton Trans.* **2019**, *48*, 1489–1503.
[28] M. D. Gholami, S. Manzhos, P. Sonar, G. A. Ayoko, E. L. Izake, *Analyst* **2019**, *144*, 4908–4916.
[29] X. Cao, Y. Wu, K. Liu, X. Yu, B. Wu, H. Wu, Z. Gong, T. Yi, *J. Mater. Chem.* **2012**, *22*, 2650–2657.
[30] O. G. Tsay, K. M. Lee, D. G. Churchill, *New J. Chem.* **2012**, *36*, 1949–1952.
[31] R. K. Pathak, V. K. Hinge, K. Mahesh, A. Rai, D. Panda, C. P. Rao, *Anal. Chem.* **2012**, *84*, 6907–6913.
[32] U. R. G. H. Agarwalla, N. Taye, S. Ghorai, S. Chattopadhyay, A. Das, *Chem. Commun.* **2014**, *50*, 9899–9902.
[33] H. Lu, H. Zhang, J. Chen, J. Zhang, R. Liu, H. Sun, Y. Zhao, Z. Chai, Y. Hu, *Talanta* **2016**, *146*, 477–482.
[34] D. Maheshwaran, T. Nagendraraj, P. Manimaran, B. Ashokkumar, M. Kumar, R. Mayilmurugan, *Eur. J. Inorg. Chem.* **2017**, *2017*, 1007–1016.
[35] D. Maheshwaran, S. Priyanga, R. Mayilmurugan, *Dalton Trans.* **2017**, *46*, 11408–11417.
[36] X. Yu, K. Wang, D. Cao, Z. Liu, R. Guan, Q. Wu, Y. Xu, Y. Sun, X. Zhao, *Sens. Actuators B: Chem.* **2017**, *250*, 132–138.
[37] A. K. Manna, J. Mondal, K. Rout, G. K. Patra, *J. Photochem. Photobiol. A: Chem.* **2018**, *367*, 74–82.
[38] T. Kim, J.-I. Hong, *ACS Omega* **2019**, *4*, 12616–12625.
[39] Y. Li, N. Shi, M. Li, *New J. Chem.* **2019**, *43*, 18517–18524.
[40] D. Das, A. Roy, S. Sutradhar, F. Fantuzzi, B. N. Ghosh, *Sens. Diagn.* **2023**, *2*, 1649–1657.
[41] D. Shao, P. Peng, M. You, L.-F. Shen, S.-Y. She, Y.-Q. Zhang, Z. Tian, *Inorg. Chem.* **2022**, *61*, 3754–3762.
[42] Z.-X. Chen, Y.-L. Wang, Q.-Y. Liu, *Inorg. Chem. Commun.* **2018**, *98*, 150–153.
[43] R. R. Nair, M. Raju, K. Jana, D. Mondal, E. Suresh, B. Ganguly, P. B. Chatterjee, *Chem. Eur. J.* **2018**, *24*, 10721–10731.
[44] R. Ghosh, S. Debnath, A. Bhattacharya, D. Pradhan, P. B. Chatterjee, *J. Inorg. Biochem.* **2022**, *233*, 111845–111854.
[45] C. N. R. Rao, R. Venkataraghavan, *Spectrochim. Acta* **1962**, *18*, 541–547.
[46] T. Steiner, *Angew. Chem. Int. Ed.* **2002**, *41*, 48–76.
[47] S. Debnath, R. R. Nair, R. Ghosh, G. Kiranmai, N. Radhakishan, N. Nagesh, P. B. Chatterjee, *Chem. Commun.* **2022**, *58*, 9210–9213.
[48] R. Ghosh, S. Luhar, S. Debnath, K. B. Patel, K. V. Baskaran, D. N. Srivastava, P. B. Chatterjee, *Sens. Actuators B: Chem.* **2024**, *406*, 135390–135398.
[49] R. Tokala, S. Sana, U. J. Lakshmi, P. Sankarana, D. K. Sigalapalli, N. Gadewal, J. Kode, N. Shankaraiah, *Bioorg. Chem.* **2020**, *105*, 104357–104407.
[50] R. Tokala, S. Bale, I. P. Janrao, A. Vennela, N. P. Kumar, K. R. Senwar, C. Godugu, N. Shankaraiah, *Bioorg. Med. Chem. Lett.* **2018**, *28*, 1919–1924.
[51] G. R. You, J. J. Lee, Y. W. Choi, S. Y. Lee, C. Kim, *Tetrahedron* **2016**, *72*, 875–881.
[52] B. J. Hathaway, A. A. G. Tomlinson, *Coord. Chem. Rev.* **1970**, *5*, 1–43.
[53] Q. Ma, X. Fang, J. Zhang, L. Zhu, X. Rao, Q. Lu, Z. Sun, H. Yu, Q. Zhang, *J. Mater. Chem. B* **2020**, *8*, 4039–4045.
[54] D. Chao, Y. Zhang, *Sens. Actuators B: Chem.* **2017**, *245*, 146–155.

Manuscript received: March 28, 2024
Version of record online: ■■, ■■

RESEARCH ARTICLE

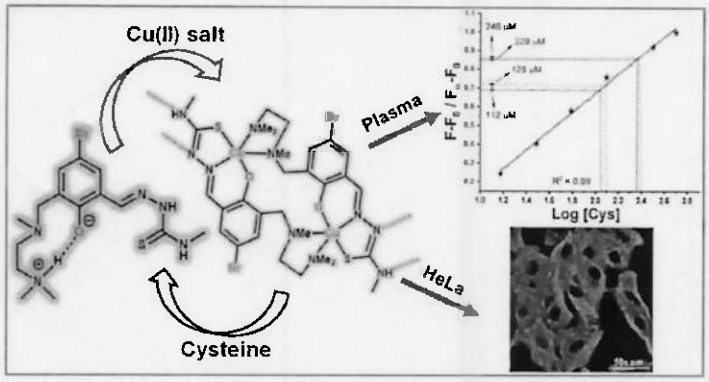

R. Ghosh, D. Pradhan, S. Debnath, A. Mansingh, N. Nagesh, P. B. Chatterjee**

1 – 11

A Hydrogen Bonded Non-Porous Organic-Inorganic Framework for Measuring Cysteine in Blood Plasma and Endogenous Cancer Cell

This article reports the synthesis of a non-luminescent one-dimensional hydrogen-bonded organic-inorganic framework (HOIF) of Cu(II) and its affinity studies with cysteine. Cysteine measurement by HOIF has been validated using a commercial dye, "Cysteine Green". The probe is suitable for measuring cysteine in plasma and bio-imaging endogenous cysteine in cancer cells.